Physics of Semiconductor Devices

SECOND EDITION

S. M. Sze

Bell Laboratories, Incorporated
Murray Hill, New Jersey

K.F. WENDT LIBRARY
UW COLLEGE OF ENGR.
215 N. RANDALL AVENUE
MADISON, WI 53706

A WILEY-INTERSCIENCE PUBLICATION

JOHN WILEY & SONS

New York • Chichester • Brisbane • Toronto • Singapore

UNIVERSITY OF WISCONSIN - MADISON
LIBRARY

Copyright © 1981 by John Wiley & Sons, Inc.

All rights reserved. Published simultaneously in Canada.

Reproduction or translation of any part of this work beyond that permitted by Sections 107 or 108 of the 1976 United States Copyright Act without the permission of the copyright owner is unlawful. Requests for permission or further information should be addressed to the Permissions Department, John Wiley & Sons, Inc.

Library of Congress Cataloging in Publication Data:

Sze, S. M., 1936-
Physics of semiconductor devices.

"A Wiley-Interscience publication."
Includes index.
1. Semiconductors. I. Title.

TK7871.85.S988 1981 537.6'22 81-213
ISBN 0-471-05661-8 AACR2

Printed in the United States of America

10 9 8 7 6 5 4 3

Contents

INTRODUCTION 1

PART I SEMICONDUCTOR PHYSICS 5

Chapter 1 Physics and Properties of Semiconductors—A Résumé 7

1.1 Introduction, 7
1.2 Crystal Structure, 8
1.3 Energy Bands, 12
1.4 Carrier Concentration at Thermal Equilibrium, 16
1.5 Carrier Transport Phenomena, 27
1.6 Phonon Spectra and Optical, Thermal, and High-Field Properties of Semiconductors, 38
1.7 Basic Equations for Semiconductor Device Operation, 50

PART II BIPOLAR DEVICES 61

Chapter 2 p-n Junction Diode 63

2.1 Introduction, 63
2.2 Basic Device Technology, 64
2.3 Depletion Region and Depletion Capacitance, 74
2.4 Current–Voltage Characteristics, 84
2.5 Junction Breakdown, 96
2.6 Transient Behavior and Noise, 108
2.7 Terminal Functions, 112
2.8 Heterojunction, 122

Chapter 3 Bipolar Transistor 133

3.1 Introduction, 133
3.2 Static Characteristics, 134
3.3 Microwave Transistor, 156
3.4 Power Transistor, 169
3.5 Switching Transistor, 175
3.6 Related Device Structures, 181

Chapter 4 Thyristors 190

4.1 Introduction, 190
4.2 Basic Characteristics, 191
4.3 Shockley Diode and Three-Terminal Thyristor, 209
4.4 Related Power Thyristors, 222
4.5 Diac and Triac, 229
4.6 Unijunction Transistor and Trigger Thyristors, 234
4.7 Field-Controlled Thyristor, 238

PART III UNIPOLAR DEVICES 243

Chapter 5 Metal–Semiconductor Contacts 245

5.1 Introduction, 245
5.2 Energy-Band Relation, 246
5.3 Schottky Effect, 250
5.4 Current Transport Processes, 254
5.5 Characterization of Barrier Height, 270
5.6 Device Structures, 297
5.7 Ohmic Contact, 304

Chapter 6 JFET and MESFET 312

6.1 Introduction, 312
6.2 Basic Device Characteristics, 314
6.3 General Characteristics, 324
6.4 Microwave Performance, 341
6.5 Related Field-Effect Devices, 351

Chapter 7 MIS Diode and CCD 362

7.1 Introduction, 362
7.2 Ideal MIS Diode, 363
7.3 Si-SiO_2 MOS Diode, 379
7.4 Charge-Coupled Device, 407

Chapter 8 MOSFET 431

8.1 Introduction, 431
8.2 Basic Device Characteristics, 433
8.3 Nonuniform Doping and Buried-Channel Devices, 456
8.4 Short-Channel Effects, 469
8.5 MOSFET Structures, 486
8.6 Nonvolatile Memory Devices, 496

PART IV SPECIAL MICROWAVE DEVICES 511

Chapter 9 Tunnel Devices 513

9.1 Introduction, 513
9.2 Tunnel Diode, 516
9.3 Backward Diode, 537
9.4 MIS Tunnel Diode, 540
9.5 MIS Switch Diode, 549
9.6 MIM Tunnel Diode, 553
9.7 Tunnel Transistor, 558

Chapter 10 IMPATT and Related Transit-Time Diodes 566

10.1 Introduction, 566
10.2 Static Characteristics, 568
10.3 Dynamic Characteristics, 577
10.4 Power and Efficiency, 585
10.5 Noise Behavior, 599
10.6 Device Design and Performance, 604
10.7 BARITT and DOVETT Diodes, 613
10.8 TRAPATT Diode, 627

Chapter 11 Transferred-Electron Devices 637

11.1 Introduction, 637
11.2 Transferred-Electron Effect, 638
11.3 Modes of Operation, 651
11.4 Device Performances, 667

PART V PHOTONIC DEVICES 679

Chapter 12 LED and Semiconductor Lasers 681

12.1 Introduction, 681
12.2 Radiative Transitions, 682

12.3 Light-Emitting Diodes, 689
12.4 Semiconductor Laser Physics, 704
12.5 Laser Operating Characteristics, 724

Chapter 13 Photodetectors **743**

13.1 Introduction, 743
13.2 Photoconductor, 744
13.3 Photodiode, 749
13.4 Avalanche Photodiode, 766
13.5 Phototransistor, 782

Chapter 14 Solar Cells **790**

14.1 Introduction, 790
14.2 Solar Radiation and Ideal Conversion Efficiency, 791
14.3 *p-n* Junction Solar Cells, 799
14.4 Heterojunction, Interface, and Thin-Film Solar Cells, 816
14.5 Optical Concentration, 830

APPENDIXES **839**

A. List of Symbols, 841
B. International System of Units, 844
C. Unit Prefixes, 845
D. Greek Alphabet, 846
E. Physical Constants, 847
F. Lattice Constants, 848
G. Properties of Important Semiconductors, 849
H. Properties of Ge, Si, and GaAs at 300 K, 850
I. Properties of SiO_2 and Si_3N_4 at 300 K, 851

INDEX **853**

The metal-overlap laterally diffused structure[65] is basically a double (parallel) Schottky diode that does not involve a p-n junction, Fig. 38i. This structure gives nearly ideal forward and reverse I–V characteristics with very short reverse recovery time. However, the process involves extra oxidation and diffusion steps, and the outer n^- ring may increase the device capacitance.

For certain microwave power generators (e.g., IMPATT diodes) one uses the truncated-cone structure,[66] Fig. 38j. The angle between the metal overhang and the semiconductor cone must be larger than 90° so that the electric field at the contact periphery is always smaller than that in the center. This angle ensures that the avalanche breakdown will occur uniformly inside the metal–semiconductor contact.

5.7 OHMIC CONTACT

An ohmic contact is defined as a metal–semiconductor contact that has a negligible contact resistance relative to the bulk or spreading resistance of the semiconductor. A satisfactory ohmic contact should not significantly perturb device performance, and it can supply the required current with a voltage drop that is sufficiently small compared with the drop across the active region of the device.

We shall first consider specific contact resistance that is the reciprocal of the derivative of current density with respect to voltage. When evaluated at zero bias, this specific contact resistance R_c is an important figure of merit for ohmic contacts:[67]

$$R_c \equiv \left(\frac{\partial J}{\partial V}\right)^{-1}_{V=0}. \tag{97}$$

For metal–semiconductor contacts with lower doping concentrations, the thermionic–emission current dominates the current transport, as given in Eq. 49. Therefore,

$$R_c = \frac{k}{qA^*T}\exp\left(\frac{q\phi_{Bn}}{kT}\right). \tag{98}$$

In deriving this equation, we have neglected the small voltage dependence of the barrier height. Equation 98 shows that low barrier height should be used to obtain small R_c.

For contacts with higher dopings, the tunneling process will dominate, and the current is given by Eq. 54a. Then

$$R_c \sim \exp\left(\frac{q\phi_{Bn}}{E_{00}}\right) = \exp\left[\frac{2\sqrt{\epsilon_s m^*}}{\hbar}\left(\frac{\phi_{Bn}}{\sqrt{N_D}}\right)\right]. \tag{99}$$

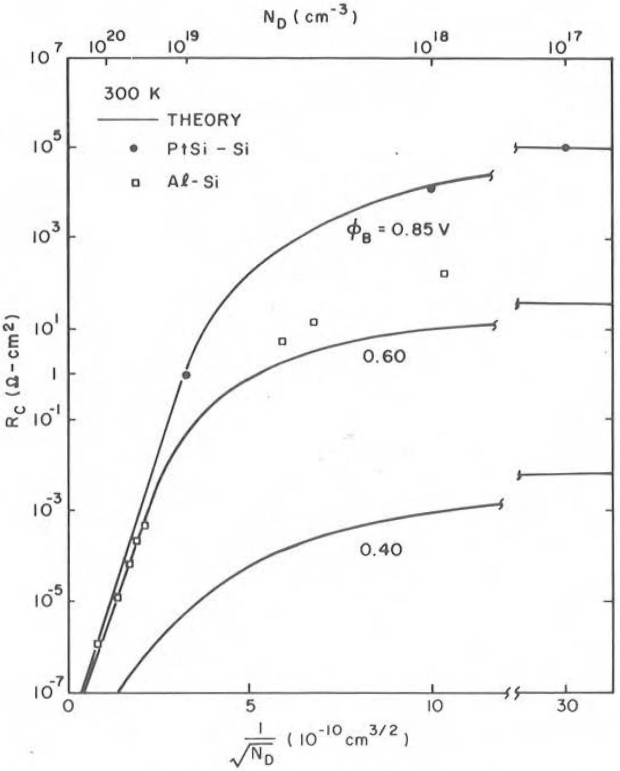

Fig. 43 Theoretical and experimental values of specific contact resistance. (After Chang, Fang, and Sze, Ref. 67; Yu, Ref. 68.)

Equation 99 shows that in the tunneling range the specific contact resistance depends strongly on doping concentration and varies exponentially with the factor $(\phi_{Bn}/\sqrt{N_D})$.

The calculated values of R_c are plotted[67,68] in Fig. 43 as a function of $1/\sqrt{N_D}$. For $N_D \geq 10^{19}\,\text{cm}^{-3}$, R_c is dominated by the tunneling process and decreases rapidly with increased doping. On the other hand, for $N_D \leq 10^{17}\,\text{cm}^{-3}$, the current is due to thermionic emission, and R_c is essentially independent of doping. Also shown in Fig. 43 are experimental data for PtSi–Si and Al–Si diodes. They are in good agreement with the calculated values.

Figure 43 shows that high doping concentration, low barrier height, or both must be used to obtain low values of R_c. And these are exactly the approaches used for all ohmic contacts (Fig. 44).

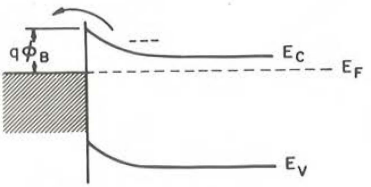

(a) LOW BARRIER HEIGHT

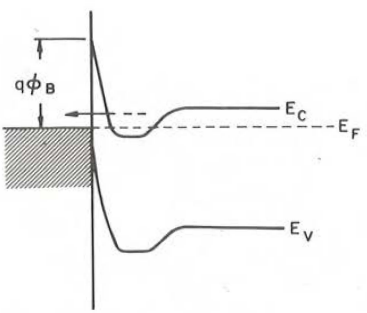

(b) HIGH DOPING

Fig. 44 Low barrier height and/or high doping for ohmic contacts.

It is difficult to make ohmic contacts on wide-gap semiconductors. A metal does not generally exist with a low-enough work function to yield a low barrier. In such cases the general technique for making an ohmic contact involves the establishment of a heavily doped surface layer such as metal–n^+-n or metal–p^+-p contact by various methods, such as shallow diffusion, alloy regrowth, in-diffusion of a dopant contained in the contact material, double epitaxy, and ion implantation. For ohmic contacts on Ge and Si, Au–Sb alloy (with 0.1% Sb) is first evaporated onto n-type semiconductors. These contacts are then alloyed at the corresponding eutectic temperature into the semiconductors under an inert gas (such as argon or nitrogen).[69] For GaAs and other III–V compound semiconductors, various technologies have been developed for the ohmic contacts.[70] A summary is listed in Table 5.

Table 5 Ohmic Contact Technology for III–V and Mixed III–V Compound Semiconductors

III–V	E_g (eV)	Type	Contact Material	Technique	Alloy Temperature (°C)
AlN	5.9	Semi-i	Si	Preform	
		Semi-i	Al, Al–In	Preform	1500–1800
		Semi-i	Mo, W	Sputter	1000
AlP	2.45	*n*	Ga–Ag	Preform	500–1000
AlAs	2.16	*n*, *p*	In–Te	Preform	150
		n. *p*	Au	Preform	160
		n, *p*	Au–Ge	Preform	700
		n	Au–Sn	Preform	
GaN	3.36	Semi-i	Al–In	Preform	
GaP	2.26	*p*	Au–Zn(99:1)	Preform, evap.	700
		p	Au–Ge	Preform	
		n	Au–Sn(62:38)	Preform	360
		n	Au–Si(98:2)	Evap.	700
GaAs	1.42	*p*	Au–Zn(99:1)	Electroless, evap.	600
		p	In–Au(80:20)	Preform	
		n	Au–Ge(88:12)	Evap.	
		n	In–Au(90:10)	Evap.	350–450
		n	Au–Si(94:6)	Evap.	550
		n	Au–Sn(90:10)	Evap.	300
		n	Au–Te(98:2)	Evap.	350–700
GaSb	0.72	*p*	In	Preform	500
		n	In	Preform	
InP	1.35	*p*	In	Preform	
		n	In, In–Te	Preform	350–600
		n	Ag–Sn	Preform, evap.	350–600 600
InAs	0.36	*n*	In	Preform	
			Sn–Te(99:1)	Preform	
InSb	0.17	*n*	In	Preform	
		n	Sn–Te(99:1)	Preform	
$GaAs_{1-x}P_x$	1.42–2.31	*p*	Au–Zn	Evap.	500
		p	Al	Evap.	500
		n	Au–Ge–Ni	Evap.	450
		n	Au–Sn	Evap.	450
$Al_xGa_{1-x}As$	1.42–2.16	*p*	Au–In	Electroplate	400–450
		p	Au–Zn	Evap.	
		p	Al	Evap.	500
		n	Au–Ge–Ni	Evap.	500
		n	Au–Sn	Evap., electroless	450–485 450
		n	Au–Si	Evap.	
$Ga_{1-x}In_xSb$	0.70–0.17	*n*	Sn–Te	Evap.	
$Al_xGa_{1-x}P$	2.31–2.45	*n*	Sn	Preform	
$Ga_{1-x}In_xAs$	1.47–0.35	*n*	Sn	Preform	
$InAs_xSb_{1-x}$	0.17–0.35	*n*	In–Te	Preform	

Appendix H

Properties of Ge, Si, and GaAs at 300 K

Properties	Ge	Si	GaAs
Atoms/cm^3	4.42×10^{22}	5.0×10^{22}	4.42×10^{22}
Atomic weight	72.60	28.09	144.63
Breakdown field(V/cm)	$\sim 10^5$	$\sim 3 \times 10^5$	$\sim 4 \times 10^5$
Crystal structure	Diamond	Diamond	Zincblende
Density (g/cm^3)	5.3267	2.328	5.32
Dielectric constant	16.0	11.9	13.1
Effective density of states in conduction band, N_C (cm^{-3})	1.04×10^{19}	2.8×10^{19}	4.7×10^{17}
Effective density of states in valence band, N_V (cm^{-3})	6.0×10^{18}	1.04×10^{19}	7.0×10^{18}
Effective Mass, m^*/m_0			
Electrons	$m_l^* = 1.64$	$m_l^* = 0.98$	0.067
	$m_t^* = 0.082$	$m_t^* = 0.19$	
Holes	$m_{lh}^* = 0.044$	$m_{lh}^* = 0.16$	$m_{lh}^* = 0.082$
	$m_{hh}^* = 0.28$	$m_{hh}^* = 0.49$	$m_h^* = 0.45$
Electron affinity, χ(V)	4.0	4.05	4.07
Energy gap (eV) at 300 K	0.66	1.12	1.424
Intrinsic carrier concentration (cm^{-3})	2.4×10^{13}	1.45×10^{10}	1.79×10^6
Intrinsic Debye length (μm)	0.68	24	2250
Intrinsic resistivity (Ω-cm)	47	2.3×10^5	10^8
Lattice constant (Å)	5.64613	5.43095	5.6533

Properties	Ge	Si	GaAs
Linear coefficient of thermal expansion, $\Delta L/L\Delta T$ (°C^{-1})	5.8×10^{-6}	2.6×10^{-6}	6.86×10^{-6}
Melting point (°C)	937	1415	1238
Minority carrier lifetime (s)	10^{-3}	2.5×10^{-3}	$\sim 10^{-8}$
Mobility (drift) (cm^2/V-s)			
	3900	1500	8500
	1900	450	400
Optical-phonon energy (eV)	0.037	0.063	0.035
Phonon mean free path λ_0 (Å)	105	76 (electron) 55 (hole)	58
Specific heat (J/g-°C)	0.31	0.7	0.35
Thermal conductivity at 300 K (W/cm-°C)	0.6	1.5	0.46
Thermal diffusivity (cm^2/s)	0.36	0.9	0.44
Vapor pressure (Pa)	1 at 1330°C 10^{-6} at 760°C	1 at 1650°C 10^{-6} at 900°C	100 at 1050°C 1 at 900°C